Chapter 1: Introduction

The Standard Model

In the past thirty years, a theory of particle interactions called the Standard Model has emerged which describes electro-magnetic, strong and weak nuclear interactions. This model is composed of a unified description of electro-magnetic and weak nuclear interactions called Electro-weak theory (which subsumes Quantum Electrodynamics, QED) and Quantum Chromodynamics (QCD), a theory describing the strong nuclear interaction.

Note: In this work, the units used will generally be natural units, that is, $c = \hbar = 1$.

Electric charges will be quoted in units of e, the magnitude of the electron's charge.

In the Standard Model, all matter is made of fundamental spin-1/2 fermions and all forces are mediated by the exchange of gauge bosons with spin-1. The fermions are divided into two types: quarks, which carry colour charge and therefore can interact via the strong force, and leptons, which do not carry colour charge. The fundamental fermions are tabulated in figure 1.1. Each fermion also has an anti-particle, denoted by placing a bar over the particle symbol. Thus, anti-up is denoted by $\bar{u}$. Although listed in the table, the existence of top quark has yet to be experimentally confirmed.

In the Standard model, matter is composed of leptons and colourless combinations of quarks called hadrons, either mesons (quark/anti-quark combinations) or baryons (three quark combinations). Three anti-quarks may form an anti-baryon. This is the quark model of hadron structure. Free quarks are not observable in this model because of the phenomenon called confinement. If an attempt is made to separate a quark from a hadron, the colour forces do not drop off with distance; instead they tend to a constant. This means that the energy in that colour field increases with the distance, so that eventually there is enough energy to liberate a quark/ anti-quark pair from the vacuum. This quark/anti-quark pair now aligns with the colour field to create two combinations with the existing quarks, so there are now two hadrons instead of a free

quark and some coloured hadron remains.

It is thought that the total number of baryons in a given interaction is conserved, giving rise to the concept of baryon number (a baryon having baryon number 1 and an anti-baryon -1). It is also thought that the total number of leptons is conserved, giving rise to the lepton quantum number. It is thought that electron, muon and tau lepton numbers are separately conserved.

The gauge bosons that carry the forces are listed in figure 1.2. The photon mediates electro-magnetic interactions, the W and Z bosons mediate weak interactions and the gluons mediate strong interactions. There are eight different varieties of gluon, each carrying a different combination of the three colour and three anti-colour charges.

Quarks:

Name	Symbol	Electric Charge	Baryon Number	Lepton Number
Up quark	*u*	+2/3	1/3	0
Down quark	*d*	-1/3	1/3	0
Charm quark	*c*	+2/3	1/3	0
Strange quark	*s*	-1/3	1/3	0
Top quark (?)	*t*	+2/3	1/3	0
Bottom quark	*b*	-1/3	1/3	0

Leptons:

Name	Symbol	Electric Charge	Baryon Number	Lepton Number
Electron	*e*	-1	0	1
e neutrino	ν_e	0	0	1
Muon	μ	-1	0	1
μ neutrino	ν_μ	0	0	1
Tau	τ	-1	0	1
τ neutrino	ν_τ	0	0	1

Figure 1.1: The fundamental fermions. There is a question mark by the top quark as its existence has not yet been experimentally confirmed. Anti-particles have opposite signed electric charge, baryon number and lepton number.

Name	Symbol	Electric Charge	Baryon Number	Lepton Number
Photon	γ	0	0	0
W boson	W	+/- 1	0	0
Z boson	Z	0	0	0
Gluon	g_j (j=1-8)	0	0	0

Figure 1.2: The gauge bosons. There are eight gluons, each carrying a different combination of colour charges.

In the standard model, the fundamental fermions are grouped into three generations, as shown in figure 1.3. It is not clear why there should be three generations as the normal matter of the universe (protons, neutrons and electrons) only requires the first. The properties of particles in the same position within a generation are similar except for the mass (which increases with increasing generation) and the lepton number or quark flavour. Thus, the muon and tau resemble heavy electrons. All three neutrinos are believed to be massless, but carry distinct electron, muon and tau lepton numbers.

1st	2nd	3rd
$\begin{pmatrix} e \\ \nu_e \end{pmatrix}$	$\begin{pmatrix} \mu \\ \nu_\mu \end{pmatrix}$	$\begin{pmatrix} \tau \\ \nu_\tau \end{pmatrix}$
$\begin{pmatrix} u \\ d \end{pmatrix}$	$\begin{pmatrix} c \\ s \end{pmatrix}$	$\begin{pmatrix} t \\ b \end{pmatrix}$

Figure 1.3: The three generations of fundamental fermions.

Open Questions In The Standard Model

The Standard Model, while comprehensive, is not yet complete. The top quark has not yet been experimentally confirmed. Searches at Fermilab have placed a lower limit on the mass of the top quark of 91 GeV at the 95% confidence level [1]. In addition, the mechanism by which the fermions acquire mass is not yet known. The favoured explanation is the Higgs mechanism [2] and the next generation of accelerators will search for the predicted Higgs bosons. It is not clear whether there is some unification of the strong and electro-weak forces at some high energy scale: this is the province of Grand Unified Theories. Finally, gravity is not included at all in the framework of the Standard Model: this is the realm of Theories of Everything. Grand Unified Theories and Theories of everything are outside the scope of this work and will not be discussed further.

More prosaic is a simple technical difficulty in calculating QCD. In QED, a perturbative expansion in the electro-magnetic coupling constant, α_{em}, is performed, with the first order diagrams containing a single factor of α_{em}, the second order diagrams containing two factors, etc. As α_{em} is small ($\approx 1/137$ at low four-momentum transfers), each succeeding order is of less significance and thus only the simpler diagrams containing a relatively small number of vertices need be considered. As the energy of the interaction increases, α_{em} also increases (e.g. to $\approx 1/128$ at LEP energies), meaning that higher order diagrams become more significant at higher energies.

In QCD, however, the strong coupling constant α_s is of order unity at low four-momentum transfers. This means that the perturbation theory approach cannot be used successfully as all possible orders of diagrams must be calculated. As the energy scale of the interaction increases, α_s decreases, meaning that perturbation theory becomes applicable. This leads to a distinction between the perturbative (or hard) region and the non-perturbative (or soft) region. In the high energy limit, α_s becomes small and the quarks appear to be unbound. This effect is known as asymptotic freedom.

The impossibility of applying perturbation theory at low energy means that the structure of hadrons, at an energy scale equal to their mass, cannot be predicted by QCD. Thus, the

formation of hadrons from asymptotically free quarks cannot be calculated in QCD and so the behaviour of hadrons at other energy scales is uncertain.

There are two approaches to this fundamental problem. One is to use lattice QCD calculations performed on computer to calculate the formation of hadrons. The other is to measure the structure at some reference scale where perturbative QCD is valid and then use perturbative QCD to evolve this behaviour to all higher scales. Lattice QCD calculations, although approaching a stage where they can be compared with some experimental features, will not be discussed further.

One of the most revealing processes to study in order to understand the composition of hadrons is lepton-hadron scattering. The lepton, believed to be point-like with no substructure, acts as a probe of the structure of the hadron. Previous experiments of this nature, for example, electron-proton scattering at SLAC [3], confirmed asymptotic freedom and the quark model of hadron structure and lead to the formulation of QCD. It has long been a goal of experimental physicists to extend the measurements of the structure of hadrons into higher energy realms where perturbative QCD can be used reliably. This also means examining the structure of the hadrons at smaller distance scale, so if new sub-structure exists, it will be seen at higher probing energies.

Previous experiments of this type have been fixed target, the lepton beam being incident upon a stationary target containing the hadrons (typically hydrogen for protons and deuterium for protons and neutrons). However, the fixed target arrangement is not an efficient way of reaching high energies in the centre-of-mass frame. For this reason, HERA (**H**adron **E**lectron **R**ing **A**nlage) has been constructed at DESY in Hamburg, Germany. This accelerator is designed to collide 30 GeV electrons (or positrons) with 820 GeV protons, giving an available energy in the centre-of-mass frame of 314 GeV, equivalent to an electron beam of 51 TeV on a stationary proton target.

Chapter 2: Physics at HERA

Introduction And General Kinematics

The basic interaction at HERA is that of electron-proton (or positron-proton) scattering. This may proceed via elastic scattering, in which both the electron and proton survive intact as shown in figure 2.1. Elastic scattering proceeds by interacting with the proton as a whole, giving information about the shape and density of the proton. Inelastic reactions, as shown in figure 2.2, are more revealing, as they break up the proton and give information about its constituents.

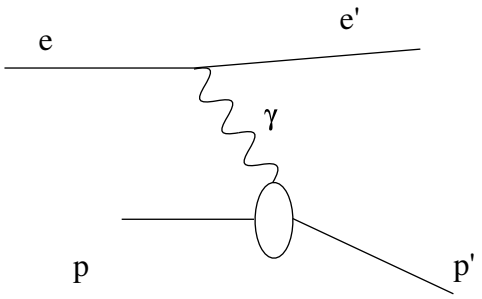

Figure 2.1: Elastic electron-proton scattering.

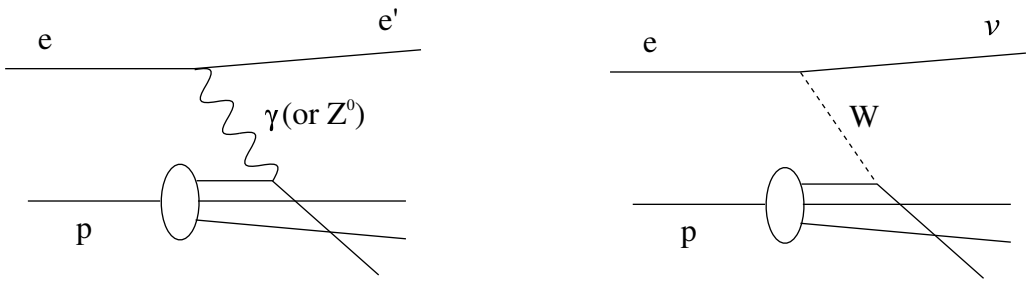

a) Neutral Current b) Charged Current

Figure 2.2: Lowest order diagrams for electron-proton inelastic scattering. a) Neutral current, mediated by photon (or Z^0), b) charged current, mediated by W.

In these reactions the virtual boson (photon, W or Z^0) emitted by the electron scatters not from the proton as a whole but from some constituent part, called a parton. Let **k** be the four-momentum of the incoming electron, **k'** the four momentum of the outgoing electron (or neutrino in the case of charged-current interactions), **p** the four momentum of the incoming proton, **p'** the four momentum of the outgoing proton and *M* the mass of the proton. The four-

momentum transfer, **q**, may then be defined as

$$\mathbf{q} = \mathbf{k} - \mathbf{k}'$$

The square of the four-momentum transfer, Q^2, (with a conventional minus sign) is then

$$Q^2 = -\mathbf{q}^2 = -(\mathbf{k} - \mathbf{k}')^2$$

The energy transferred by the exchanged particle in the rest frame of the proton, ν, is then defined as

$$\nu = \frac{\mathbf{p} \cdot \mathbf{q}}{M}$$

The variable x (also called Bjorken x) is the fraction of the proton's four-momentum taken by the interacting parton and is given by

$$x = \frac{Q^2}{2M\nu}$$

and Bjorken y, a useful variable related to x and Q^2, is defined as

$$y = \frac{\mathbf{p} \cdot \mathbf{q}}{\mathbf{p} \cdot \mathbf{k}}$$

Deep Inelastic Scattering

One of the great successes of the quark-parton model and its generalisation, QCD, is an explanation of the phenomenon now known as Bjorken scaling [4]. It was observed that electron-proton scattering in the deep inelastic region, Q^2>10 GeV^2, could be explained by considering the process as an elastic scatter from a point-like parton with four-momentum fraction x within the proton. This meant that the cross-section as a function of Q^2 behaved in the same way as scattering from a point charge for fixed x. In fact, scaling is only exact for the

$x \approx 0.25$ region. Outside this region the simple picture of figure 2.2 begins to break down. The reasons for this will discussed in the section entitled 'Parton Distributions And Scaling Violations'.

Form Factors And Structure Functions

QED gives the differential cross section for elastic electron-muon scattering as [5]

$$\frac{d\sigma}{d\Omega}\,(pointlike) = \frac{\alpha_{em}^2}{4E^2\sin^4\left(\frac{\theta}{2}\right)}\,\frac{E'}{E}\left[\cos^2\left(\frac{\theta}{2}\right) - \frac{q^2}{2M^2}\,\sin^2\left(\frac{\theta}{2}\right)\right]$$

where Ω is solid angle, α_{em} is the electro-magnetic coupling constant, E and E' are the energy of the incoming and outgoing electron respectively and θ is the angle of the scattered electron relative to its incoming direction in the rest frame of the muon as shown in figure 2.3. M is the mass of the target and q^2 is the squared four-momentum of the exchanged photon as before. This formula is called the Mott cross-section and applies to the elastic electro-magnetic scattering of any two point-like spin 1/2 particles, one of which is massive and the other light.

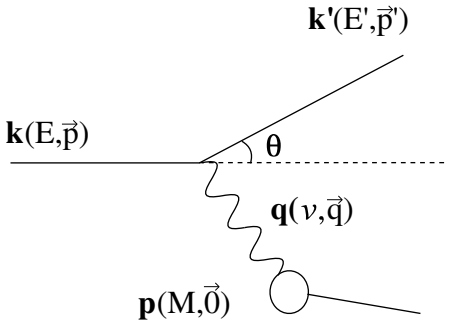

Figure 2.3: Scattering of point-like spin 1/2 particles. The upper particle is assumed light, the lower particle massive.

The proton is a spin 1/2 object but it is not point-like, having some diffuse structure in space. However, the Mott cross-section formula above may be used as the basis for the electron-proton calculation by replacing the muon current by the proton current. The muon current J_α is defined as

$$J_\alpha = \overline{u}_{\mu 2}\gamma_\alpha u_{\mu 1}$$

where γ_α are the Dirac gamma matrices. The current for the proton can be expressed in a similar way, but the gamma matrices must be replaced with a more general function that leaves the current as a Lorentz invariant. The most general form is given by

$$J_\alpha = \overline{u}_{p2}\left[f_1(Q^2)\gamma_\alpha + \frac{\kappa}{2M} f_2(Q^2) i\sigma_{\alpha\beta}\gamma^\beta + f_3(Q^2) q_\alpha\right] u_{p1}$$

where f_1, f_2 and f_3 are unknown proton elastic form factors, κ is the anomalous magnetic moment of the proton, $\sigma_{\alpha\beta}$ is related to the commutator for the gamma matrices ($\sigma_{\alpha\beta}=[\gamma_\alpha,\gamma_\beta]/2i$) and q_α are the components of the four-momentum of the exchanged photon.

The f_1 term has the same form as for a point-like charge (such as the muon) but is multiplied by a form factor that is a function of Q^2. This describes the distribution of charge within the proton. The f_2 term represents the anomalous magnetic moment of the proton, the normal magnetic moment being included in the f_1 term. The f_3 term violates parity conservation and does not enter in electromagnetic electron-proton scattering. At low Q^2, the scattering formula reduces to that for a particle with charge $+e$ and with magnetic moment $1+\kappa$. Hence, $f_1(0)=1$ and $f_2(0)=1$. If the proton were a point-like particle, f_1 would be unity for all Q^2 and κ would be zero.

Two combinations of the form factors are made to simplify experimental extraction. These are the electric and magnetic elastic form-factors, G_E and G_M, defined as

$$G_E(Q^2) = f_1(Q^2) + \frac{\kappa q^2}{4M^2} f_2(Q^2)$$

$$G_M(Q^2) = f_1(Q^2) + \kappa f_2(Q^2)$$

This gives the scattering cross-section as

$$\frac{d\sigma}{d\Omega} = \frac{\alpha_{em}^2}{4E^2 \sin^4\left(\frac{\theta}{2}\right)} \frac{E'}{E} \left[\frac{G_E^2 + \tau G_M^2}{1 + \tau} \cos^2\left(\frac{\theta}{2}\right) + 2\tau G_M^2 \sin^2\left(\frac{\theta}{2}\right) \right]$$

where τ is defined as $Q^2/4M^2$. This is known as the Rosenbluth formula.

For elastic scattering, $Q^2=2M\nu$ (i.e. $x=1$). This is not the case for inelastic scattering, as the proton breaks up and so the form factors become functions of ν as well as Q^2. Hence,

$$\frac{d\sigma}{d\Omega} = \frac{\alpha_{em}^2}{4E^2 \sin^4\left(\frac{\theta}{2}\right)} \frac{E'}{E} \left[W_2(\nu , Q^2) \cos^2\left(\frac{\theta}{2}\right) + 2W_1(\nu , Q^2) \sin^2\left(\frac{\theta}{2}\right) \right]$$

where W_1 and W_2 are the inelastic structure functions.

Bjorken's Scaling Hypothesis And The Parton Model

At $Q^2>3$ GeV^2, the proton stops looking like a diffuse object and instead looks like a collection of point-like objects, called partons. This is known as Bjorken's scaling hypothesis. These partons have now been identified with the quarks and gluons of QCD. Hence the structure functions can be reduced to

$$2W_1 = \frac{Q^2}{2m^2} \delta\left(\nu - \frac{Q^2}{2m} \right)$$

$$W_2 = \delta\left(\nu - \frac{Q^2}{2m} \right)$$

as the photon is assumed to be scattering from a point-like particle of mass m. The point-like structure functions do not depend upon Q^2 and ν independently, but on the ratio $Q^2/2m\nu$.

If the interaction is between an electron and a quark with momentum fraction x (i.e. mass fraction $m=xM$), the two dimensionless structure functions F_1 and F_2 are functions of x only and are given by

$$F_1(x) = MW_1(\nu , Q^2)$$

$$F_2(x) = \nu W_2(\nu , Q^2)$$

where $x=Q^2/2M\nu$ as before. Hence

$$F_1(x) = \frac{1}{2x} F_2(x)$$

(generally true if the components of the target have spin 1/2). This is known as the Callan-Gross relation.

Parton Distributions And Scaling Violations

The dimensionless structure functions F_1 and F_2 can be related to the parton (quark and gluon) distributions in the proton. As the gluon carries no electromagnetic charge and the photon carries no colour charge, photons and gluons cannot interact directly. Hence the structure function F_2 may be expressed as a sum over the quark distributions in the proton, giving

$$F_2(x) = \sum_i e_i^2 x q_i(x)$$

where the sum i is over the quark and anti-quark flavours, e_i are the quark charges and $q_i(x)$ are the quark distributions (the chance of finding a quark of flavour i with a momentum fraction x).

However, in QCD, the situation is more complicated as instead of seeing a quark with momentum fraction x, the quark can radiate a gluon and therefore have a lower momentum fraction. The chance of resolving this gluon from the parent quark depends upon the distance scale with which the proton is probed (i.e. $1/Q^2$). This is illustrated in figure 2.4.

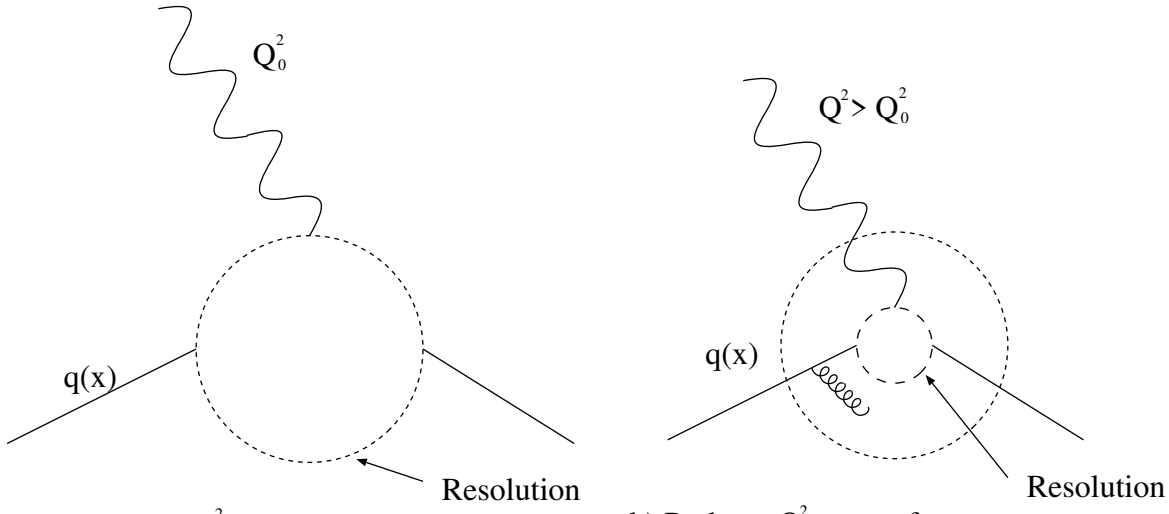

Figure 2.4: The quark structure of the proton as seen by a virtual photon as Q^2 increases. From [5].

This effect leads to scaling violations which are predicted by QCD and have been confirmed by experiment. Thus, $F_2(x)$ is replaced by $F_2(x,Q^2)$. The quark distributions are also functions of both x and Q^2. Using QCD, the variation is found to be logarithmic with Q^2. Given the quark distributions at some reference scale, $q_i(x,Q^2_0)$, the Altarelli-Parisi equation [6] may be used to evolve the distributions to a different scale, $Q^2 > Q^2_0$. Hence,

$$\frac{\mathrm{d}q(x\,,\,Q^2)}{\mathrm{d}\,\log Q^2} = \frac{\alpha_s(Q^2)}{2\pi}\int_x^1 \frac{\mathrm{d}z}{z}\, q(z\,,\,Q^2) P_{qq}\left(\frac{x}{z}\right)$$

where $\alpha_s(Q^2)$ is the strong coupling constant and $P_{qq}(x/z)$ represents the probability of a quark emitting a gluon. The expression predicts that the chance of finding a quark with momentum fraction x also has to include the chance of finding a quark, originally with momentum fraction z, that has radiated a gluon. P_{qq} is calculable in QCD. Figure 2.5 shows the deviations from scaling for F_2 compared with calculations by Gluck, Reya and Vogt [7].

Figure 2.5: Comparison between structure function data from SLAC, EMC and BCDMS with leading order and higher order predictions of Gluck, Reya and Vogt. The dotted higher order curves are an alternative calculation of the charm quark contribution. From [7].

The neutral-current cross-section for electron proton scattering in leading-order electro-weak theory is given by

$$\frac{d^2\sigma^{nc}}{dxdQ^2} = \frac{4\pi\alpha_{em}^2}{xQ^4}\left[y^2xF_1^{nc}(x\,,\,Q^2) + (1-y)F_2^{nc}(x\,,\,Q^2) - \left(y - \frac{y^2}{2}\right)xF_3^{nc}(x\,,\,Q^2)\right]$$

and the charged current cross section by

$$\frac{d^2\sigma^{cc}}{dxdQ^2} = \frac{G_f^2M_W^4}{\pi x\left(M_W^2+Q^2\right)^2}\left[y^2xF_1^{cc}(x\,,\,Q^2) + (1-y)F_2^{cc} + \left(y - \frac{y^2}{2}\right)xF_3^{cc}(x\,,\,Q^2)\right]$$

where G_f is the Fermi constant and M_W is the mass of the W boson.

The Callan-Gross relation, which is exact in the parton model, is now only approximately true and the longitudinal structure function F_L (defined as F_2-$2xF_1$) is non-zero at low x.

Gluons In The Proton And The Momentum Sum Rule

The structure function F_2 discussed above does not describe the full structure of the proton as, from QCD, the presence of quarks implies a cloud of virtual gluons. The presence of the gluons has been neglected except when considering the effect they have on the spectrum of the quark distributions in x. The gluons can be neglected because the virtual photon probe does not couple to the gluonic content of the proton directly. However, for hadron-hadron interactions, the gluons of one hadron must be considered as partons in their own right because they can interact strongly with partons from the other hadron. Therefore, each of the gluon colour combinations has its own gluon density $g_j(x,Q^2)$ where the subscript j represents the gluon colour and runs from 1 to 8.

It is difficult to measure the gluon distributions experimentally for the same reason that the gluon contribution could be neglected in the earlier description of deep inelastic scattering. However, an inference from the measured quark distributions is

$$\sum_{flavours} \sum_{colours} \int_0^1 \mathrm{d}x \; xq(x\,,\,Q^2) \;+\; \sum_{colours} \int_0^1 \mathrm{d}x \; xg(x\,,\,Q^2) = 1$$

for all values of Q^2, where q represents the quark and anti-quark distributions and g represents the gluon distributions. This expression states that the sum over all momentum fractions must be unity because the whole momentum of the proton must be carried by its constituents. This is known as the momentum sum rule.

Initially, the proton was believed to consist of three valence quarks and a sea of virtual gluons and virtual quark/anti-quark pairs with most of the proton momentum carried by the valence quarks. However, experimental measurements showed that about half of the momentum is actually by the quarks, the rest being carried by the gluons [9].

The Spin Of The Proton

In the simple parton model, the spin of the proton is the vector sum of the spins of the three valence quarks. Measurements in neutron and hyperon decays [10] show that the up and down quarks alone do not carry all of the nucleon spin, which suggests that the sea quarks may also contribute to the spin of the nucleon. Measurements by the E.M.C. collaboration [11] disproved this hypothesis by finding that the net contribution of the quarks to the nucleon spin was zero within errors. Hence, the sea quark contribution must in fact be large and negative to cancel out the valence quark contributions.

The zero net contribution of the quark spins to the spin of the nucleon may be explained using QCD [12]. Since the quarks do not carry the spin of the nucleon as predicted by the simple parton model, QCD must be used to explain which of the constituent parts of the nucleon carry the spin. This is done using the sum rule

$$\frac{1}{2}\Delta q + \Delta g + L_z = \frac{1}{2}$$

where Δq is the contribution from the quarks, Δg is the contribution from the gluons and L_z is the contribution from the orbital angular momenta of the nucleon's constituents. The net contribution from the gluons, Δg, is also found to be zero and therefore the spin must be carried by the angular momentum of the constituents. In this model the gluons carry 50% of the nucleon's linear momentum and 40% of the orbital angular momentum.

Photoproduction At HERA

Introduction

Photoproduction experiments were originally performed at fixed-target experiments using a beam of real photons incident on a stationary target (typically hydrogen or deuterium). At HERA, electron-proton scattering proceeds by the electron emitting a virtual photon which then interacts with the proton. Therefore the electrons are effectively a source of virtual photons. The regime where the photon is almost real, $Q^2 \approx 0$, is called the photoproduction region. There is a continuous transition between the photoproduction region and the deep inelastic scattering region at $Q^2 \approx 3-5$ Gev^2.

Using the electron as a source of virtual photons, the electron-proton cross section may be expressed as

$$\frac{d\sigma_{ep}}{dz dQ^2} = \frac{df_{\gamma/e}}{dz dQ^2}\,\sigma_{\gamma p}(E_\gamma)$$

where z is the fraction of the electron's energy taken by the emitted photon, E_γ is the energy of the virtual photon (given by $E_\gamma = zE_e$), $\sigma_{\gamma p}$ is the real photon-proton cross section and $f_{\gamma/\varepsilon}$ is the flux distribution of virtual photons. Assuming that the photons are almost real (i.e. that the photons are transversely polarised), the differential flux distribution may be written as

$$\frac{df_{\gamma/e}}{dz dQ^2} = \frac{\alpha_{em}}{2\pi}\,\frac{1 + (1 - z)^2}{zQ^2}$$

by using the Weizsacker-Williams formula for $f_{\gamma/e}$ [13]. The virtual photons are emitted predominantly with low values of z and Q^2. When integrating over Q^2, the limits must be specified (i.e. $Q^2_{\min}$ to $Q^2_{\max}$) to avoid the singularity at $Q^2 = 0$. The differential cross section $ep \rightarrow e'X$ is then

$$\frac{d\sigma}{dz}\,(ep \rightarrow e'X) = d\sigma_{\gamma p}\,\frac{\alpha_{em}}{2\pi}\,\frac{1 + (1 - z)^2}{z}\,\ln\frac{Q^2_{max}}{Q^2_{min}}$$

The limitations of the Weizsacker-Williams approach and a more general discussion of photon flux calculations may be found in [14], [15] and [16].

As there is a significant contribution from almost real photons, the way in which these photons interact with the proton must be considered. The interactions can be split into two classes. The first class, known as direct (figure 2.6), is where the photon interacts with one of the partons from the proton. The second class, known as resolved (figure 2.7), is where the photon fluctuates into a hadronic system and then interacts with the proton.

The resolved processes may be further divided into anomalous interactions (figure 2.7), where the photon becomes a quark/anti-quark pair, and vector meson interactions (figure 2.8), where the photon fluctuates into a system resembling a vector meson (ρ^0,ω,ϕ,J/ψ, etc.) with the same spin-parity as the photon ($J^{PC}=1^{--}$). This system contains a quark/anti-quark pair and an associated cloud of gluons. The division of the events into direct and resolved is distinct and physical, whereas the division of resolved interactions into anomalous and VMD is a continuous one, motivated by theoretical constraints.

The nomenclature of photoproduction processes described in this thesis is based on the agreed nomenclature of the photoproduction working group at the 1993 Durham QCD workshop [17]. It differs slightly from some previously published papers, for example [18], and removes the confusion arising from different uses of the term "point-like", which was used to describe direct interactions by some authors and the anomalous contribution to resolved interactions by others.

Even though the cross-section for resolved processes is reduced by a factor of α_{em} compared with direct processes, the cross section for the parton-level interactions is significantly higher when the partons can interact by the strong force. Therefore both direct and resolved interactions must be considered.

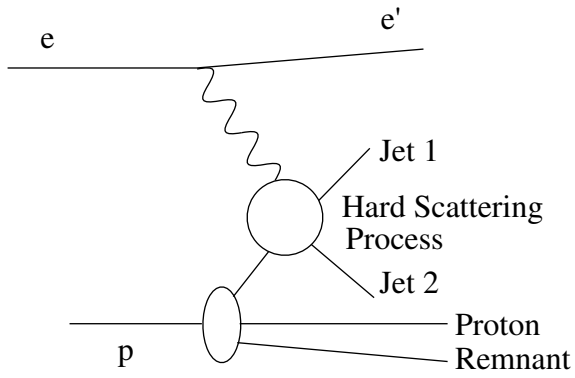

Figure 2.6: A direct interaction, in which the photon interacts directly with partons from the proton.

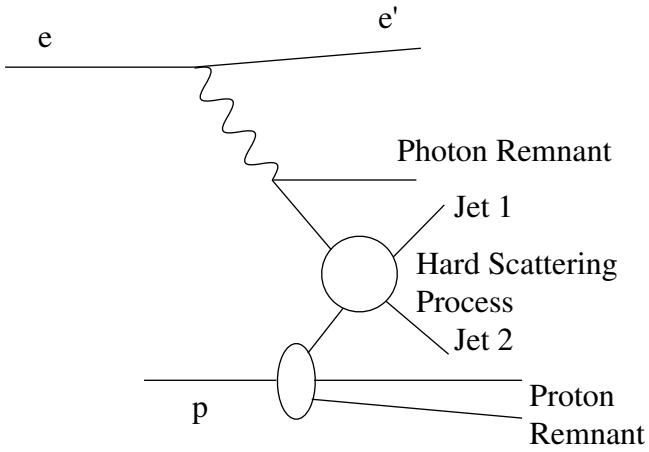

Figure 2.7: An anomalous interaction, in which the photon fluctuates to a quark-anti-quark pair.

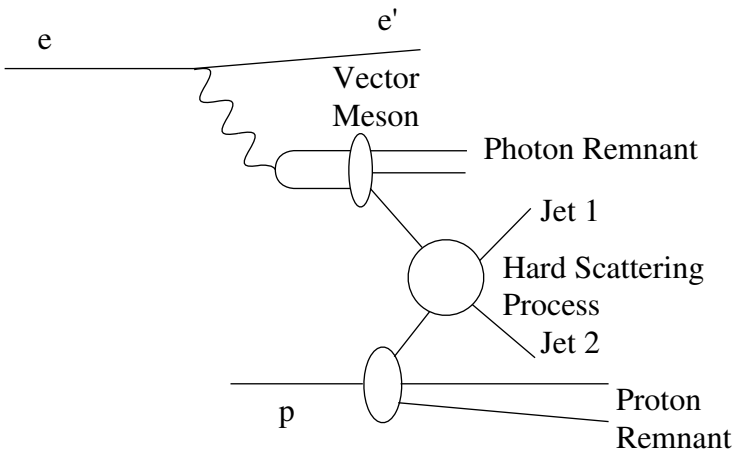

Figure 2.8: A vector meson interaction, in which the photon fluctuates to a vector meson with the same quantum numbers as the photon.

In previous experiments ([19] and the references contained therein), it was found that the data could be described very well by considering only vector meson interactions. This lead to the Vector Meson Dominance (VMD) model, where the photon is considered to be a mixture of ρ^0,ω,ϕ vector mesons [19]. The proportion of each vector meson in the mixture is given by the ratio of the couplings of the photon to the vector meson as predicted by the effective charge of the quark content of the meson. This gives the ratio ρ^0:ω:ϕ as 9:1:2. This may be extended to include contributions from all other know vector mesons, which is known as the Extended Vector Meson Dominance model (EVMD) [20]. Another refinement of the basic VMD model includes a complete Veneziano spectrum of vector mesons: this is General Vector Meson Dominance (GVMD) [21].

The power of the VMD model in explaining the fixed target data may be illustrated by the Σp_T^2 spectrum of single charged particles produced by photoproduction in WA69 [18], shown in figure 2.9. The data for photon-proton scattering are scaled up by a factor of approximately 200 and compared with the data for pion-proton scattering. Only at values of Σp_T^2 above 3 GeV^2 does the photon begins to look different from a hadron.

Figure 2.9: Σp_T^2 of charged particles produced in photon-proton collisions (points) compared with those produced in pion proton collisions (open points). The histogram is a Monte Carlo prediction and the triangular points are the direct contribution. From [18].

Direct Photon Interactions

There are only two different Feynman diagrams for direct photon interactions in lowest order. These are QCD Compton scattering and Boson-Gluon Fusion, shown in figure 2.10a and figure 2.10b respectively. In these interactions there is no visible structure to the photon as it always interacts with its full energy and no photon remnant is produced. Calculations of the cross-sections for direct processes appear in [22].

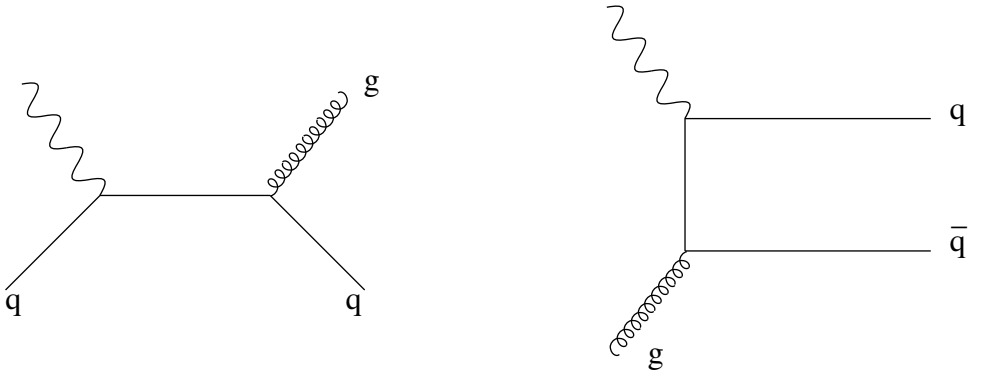

a) QCD Compton b) Boson-Gluon Fusion

Figure 2.10: Feynman graphs for hard scattering sub-processes in direct photoproduction. a) QCD Compton b) Boson-Gluon Fusion.

Resolved Photon Interactions And Parton Distributions In The Photon

In resolved interactions, the photon fluctuates into a quark/anti-quark pair (anomalous) or a vector meson (VMD). Anomalous interactions can be calculated using perturbative QCD although there is a question of how low in scale perturbation theory may be applied as the strong coupling constant, α_s, becomes large. The VMD component cannot be calculated in perturbation theory and so parameterisations must be made based on experimental measurements. This has been done using Regge theory [23] to produce fits to the fixed-target data, for example in [24].

Resolved processes can be considered to be due to quark distributions $q^{\gamma}_{i}(x)$ and gluon distributions $g^{\gamma}_{j}(x)$ inside (i.e. the photon having fluctuated to a state containing a quark or gluon) the photon with x being the fraction of the photon's four-momentum taken by the parton. This is necessary to perform perturbative QCD calculations to determine the chance of finding a quark or a gluon in the photon.

However, the momentum sum rule does not apply in the same way for the photon as it does for the proton because the photon is not composed of quarks and gluons and must fluctuate to a quark/anti-quark state before interacting via the strong force. Thus, although the sum rule must apply when the photon has fluctuated, it is possible that the photon will not fluctuate at all and therefore none of the momentum will be carried by partons. It is possible to represent the chance of the photon interacting directly by including a spike in the photon structure functions at x=1.

The structure functions F^{γ}_{1}, F^{γ}_{2} for electron-photon scattering (where the structure of a real photon is probed by a virtual photon radiated from an electron) are defined in exact analogy with the electron-proton case. This gives the differential cross-section as

$$\frac{d^2\sigma}{dxdQ^2}(e\gamma\rightarrow eX) = \frac{4\pi\alpha_{em}^2}{xQ^4}\left[y^2xF_1^{\gamma}(x\,,\,Q^2) + (1-y)F_2^{\gamma}(x\,,\,Q^2)\right]$$

where x,y are Bjorken x and y for the real photon and Q^2 is the four-momentum transfer. F_1 may be found using the Callan-Gross relation

$$2xF_1^{\gamma} = F_2^{\gamma}$$

and F^{γ}_2 is given by

$$F_2^{\gamma}(x, Q^2) = \sum_i xe_i^2 q_i^{\gamma}(x, Q^2)$$

where e_i are the quark charges, $q_i^{\gamma}(x, Q^2)$ are the quark distributions in the photon and the sum i is over quark and anti-quark flavours.

The parton distributions may be parameterised by making some theoretical assumptions (for example, that the up, down, anti-up and anti-down distributions are the same). Several sets of parameterisations are available, including the three by Levy, Abramowicz and Charchula (LAC)[25], the one by Gordon and Storrow [26] and the one by Gluck, Reya and Vogt (GRV) [27].

The LAC sets are leading order and follow the approach of the earlier work by Drees and Grassie [28]. The parton distributions are obtained by taking the distributions measured at a reference value of $Q^2=Q^2_0$ and evolving them to higher values of Q^2 using the Altarelli-Parisi equation. The anti-quark distributions are assumed to be the same as the quark distributions and a division between VMD and anomalous contributions is made inside the parton distributions. The reference scale Q^2_0 is taken to be 1 GeV^2 and 4 GeV^2 for sets III and I respectively. Set II is also produced with reference scale 4 GeV^2 but using one less free parameter. The results of the parameterisation for F^{γ}_2 are shown in figure 2.11. The sharp discontinuities are due to the inclusion of the charm quark distribution when the mass of the photon-photon system exceeds 3 GeV.

Gordon and Storrow also take a mixture of hadronic and quark-parton model pieces in the quark and gluon distributions. The calculations are in next-to-leading order as well as leading order. Q^2_0 is taken to be 5.3 GeV^2 because for lower values the contributions from higher order terms may become significant.

GRV use the very low value of Q^2_0=0.25 GeV^2 in an attempt to generate the behaviour of the parton distributions dynamically from input distributions that are VMD motivated. Figure 2.12 shows a comparison of the GRV predictions with measurements from TPC/2γ and PLUTO.

Care must be taken to avoid double counting of diagrams when calculating VMD and anomalous contributions separately. The parameterisations of LAC and Gordon-Storrow avoid this by having the parton distributions as a sum of VMD and anomalous parts and then fitting them to data. This is essentially a phenomenological approach. GRV avoid the problem by starting with VMD and evolving all parton distributions from this dynamically.

Schuler and Sjostrand outline an alternative approach to the other structure function parameterisations in [29]. In this approach, the total cross section is decomposed into direct, anomalous and resolved components, giving the total cross section as

$$\sigma^{\gamma p}_{tot}(s) = \sigma^{\gamma p}_{direct}(s) + \sigma^{\gamma p}_{VMD}(s) + \sigma^{\gamma p}_{anom}(s)$$

A sharp cutoff is then imposed at transverse momentum, p_T=p_0, below which all interactions are assumed to be VMD and above which all interactions are considered to be the sum of direct and anomalous. Therefore, the parton distributions for anomalous and VMD processes are considered separately and double counting is avoided. However, such a sharp cutoff is somewhat unphysical as a gradual change from VMD to perturbative QCD is expected.

Figure 2.11: Comparison of the predictions of the LAC parameterisations for Q^2_0=1 GeV^2 (dashed line), Q^2_0=4 GeV^2 (full line) and the Drees and Grassie parameterisation (dotted line) with the measurements of F^{γ}_2 as a function of x in bins of Q^2. From [25].

Figure 2.12: GRV predictions (solid curves) for F_2^{γ} compared with VMD-inspired parameterisations (dashed and dashed-dotted curves). The data from PLUTO (x) and TPC/2γ (+) are also shown The values of Q^2 are in GeV^2. From [27].